ACS OMEGA

http://pubs.acs.org/journal/acsodf

Article

Experimental and Computational Studies of Azo Dye-Modified Luminol Oligomers: Potential Application in Lithium Ion Sensing

Neetika Singh, Elham S. Aazam, and Ufana Riaz*

Cite This: *ACS Omega* 2021, 6, 27833−27841

Read Online

ACCESS | Metrics & More | Article Recommendations | Supporting Information

ABSTRACT: With a view to design novel conjugated oligomers via a facile technique for its possible application in sensors, the present work reports oligomerization of Bismarck Brown (BB) dye with luminol. The structure was confirmed via IR studies, while the electronic transitions were confirmed by UV−visible studies. Morphological studies were carried out via SEM. Computational studies were carried out using the DFT method with a B3LYP 6-311G(d) basis set to investigate the optimized geometry, band gap, and vibrational and electronic transitions data. The HOMO−LUMO energies showed significant reduction in the band gap upon increasing the content of BB dye. The computational IR and UV spectra were noticed to be in close agreement with the experimental results. Spectrophotometric determination of Li ion was attempted using lithium chloride and a lithium carbonate drug commonly used in the treatment of bipolar disorder. The detection limit was noticed to be as low as 5.1×10^{-6} M, which could be used to design a Li ion sensor.

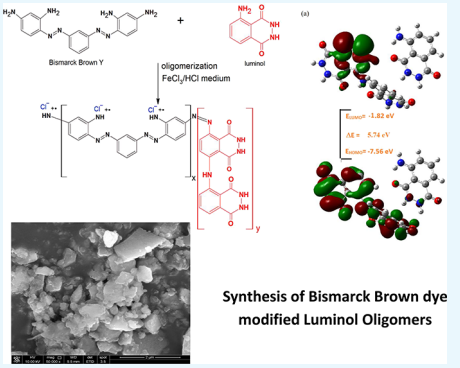

INTRODUCTION

One of the major challenges in the area of molecular electronics is the design of novel optoelectronic materials.[1] Research based on conducting polymers (CPs) has become one of the most vital fields in functional materials due to their outstanding properties such as flexibility, redox switching, low cost, lightweight, etc.[2,3] Significant progress has been made in designing CPs via chemical synthesis to achieve tunable electrochemical properties applicable in batteries,[4] super capacitors,[5] fuel cell electrodes,[6] biosensors,[7] desalination systems,[8] drug release,[9] ion-sensitive electrodes,[10] and electro-chemo-mechanical actuators.[11] However, obtaining polymers with controlled architecture is difficult because of the high molecular weight of these polymers due to the development of a cross-linked structure, which ultimately results in insolubility and intractability.[12,13]

In this regard, the design of low-molecular-weight oligomers/co-polymers of CPs has been extensively investigated as it helps in achieving controlled morphology besides ease of tuning of the electrochemical characteristics.[14] Azo-based dyes exhibit multi-functionality and extended delocalization of the π-electronic clouds, and hence the tailoring of these dye moieties with CPs imparts multi-functionality to the polymeric architecture, which can help in attaining various kinds of redox states.[14,15] The chemical synthesis of conjugated polymers in the presence of azo dyes has been investigated in the literature.[16] Valtera et al.[15] used dyes such as Acid Red 1, Orange G, and Sunset Yellow as soft templates for the synthesis of naphthyl phenyl diazene skeletons for the preparation of PPy in aqueous solution. Lei et al.[16] explored the structural properties of indigo-based polythiophene (PTh), while Kaur et al.[17] reported 4-dicyanomethylene-2-methyl-6-*p*-dimethyl aminostyryl-4H (DCM) pyran dye-doped thiophene-based conjugated polymers. Wei et al.[18] synthesized polycarbazole (PCz)-conjugated polymers via the incorporation of intense light-absorbing organic dyes—dicyanovinyl group (DCN) and diethyl thiobarbituric acid (DTA) photovoltaic applications. Jung et al.[19] synthesized CPs composed of isoindigo with 2-decyltetradecane (DT) and bithiophene with/without fluorination used in high-performance organic solar cells.

We have earlier reported the polymerization/co-polymerization of luminol with CPs such as poly(*o*-phenylenediamine) (POPD),[20] poly(*o*-anisidine) (PoA),[21] poly(α-naphthylamine) (PNA),[22] and PCz.[21]

To the best of our knowledge, no work has been reported on the oligomerization of luminol with Bismarck Brown (BB) dye.[23] BB dye has been mostly investigated as a dye pollutant and to date, we do not find any literature based on the utilization of the multi-functionality of BB dye for the design of CPs with enhanced fluorescence characteristics. Hence, the present work reports the synthesis and the design of BB dye oligomers using luminol in various molar ratios via a chemical polymerization method. The synthesized oligomers were

Received: July 1, 2021
Accepted: September 17, 2021
Published: October 13, 2021

Scheme 1. (I–III) Oligomerization of PLu with OBB Dye

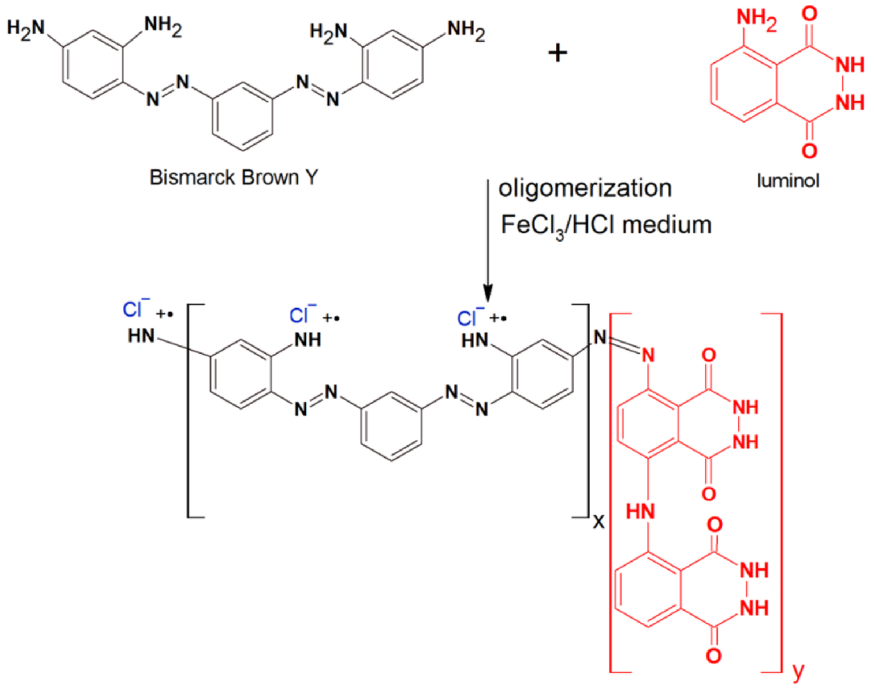

I. Copolymerization containing higher no of Luminol units (OBB/PLu-20/80)

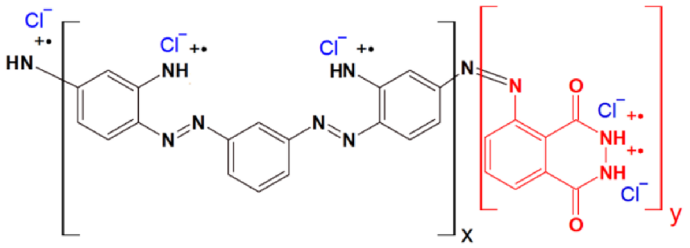

II. Copolymerization containing equal no of Bismarck and Luminol units (OBB/PLu-50/50)

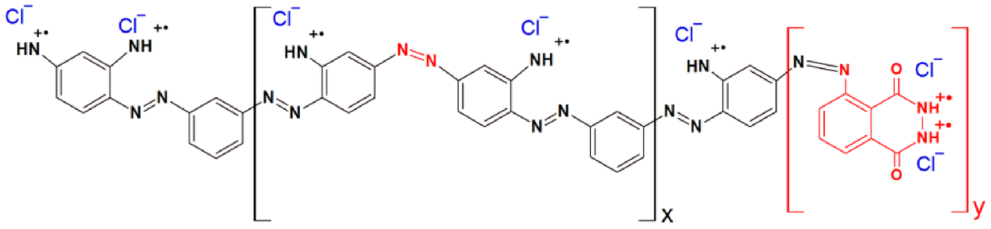

III. copolymerization containing higher no of luminol units (OBB/PLu-20/80)

characterized using FTIR, UV–visible, XRD, and TEM studies. Computational DFT studies were carried out using the DFT/B3LYP method with the 6-311G(d) basis set to compare and verify the experimental data. Lithium chloride was chosen as a model compound along with a lithium carbonate drug, which is widely used to treat mental disorders such as bipolar disorder.[24] The drug has a narrow therapeutic index, and long-term effects can increase the chances of toxicity.[24] Hence, a technique is required that can provide rapid measurement of lithium in an accurate manner to improve the compliance of lithium treatment with possible reduction in toxicity. We have used a spectrophotometric method for the detection of lithium in salt with the view of possibly fabricating a device for simple measurement of lithium doses.

RESULTS AND DISCUSSION

The solubility of the OBB/PLu oligomers is provided in the Supporting Information as Table S1. The oligomers were noticed to be soluble in DMSO, DMF, and NMP. The viscosity average molecular weight was calculated as per the method reported in our earlier studies.[25,26] The intrinsic viscosity was measured as per the method reported in our previous studies.[16,17] The value of intrinsic viscosity was

https://doi.org/10.1021/acsomega.1c03459
ACS Omega 2021, 6, 27833–27841

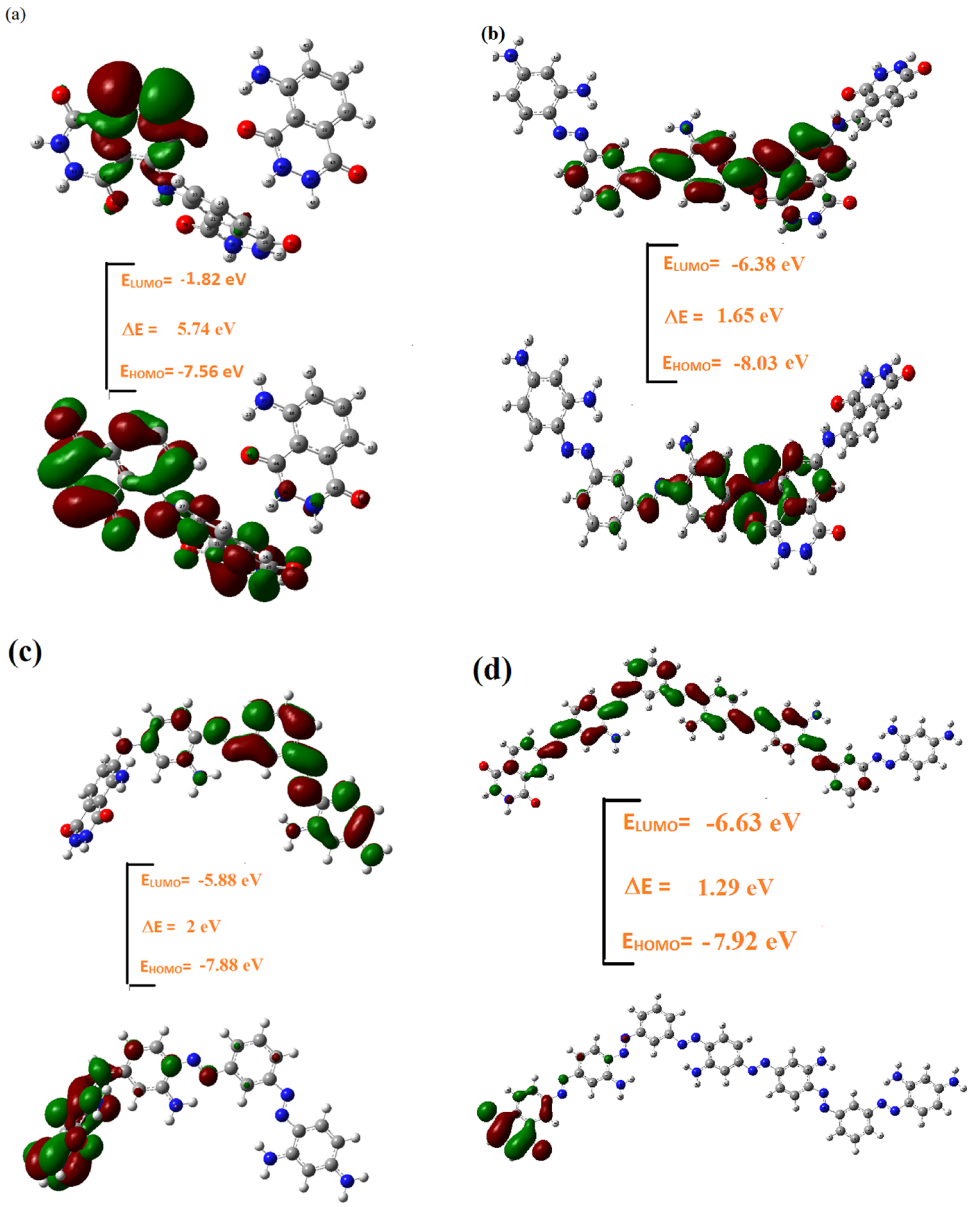

Figure 1. HOMO−LUMO energies of (a) PLu, (b) OBB/PLu-20/80, (c) OBB/PLu-50/50, and (d) OBB/PLu-80/20.

calculated to be 0.78 for OBB/PLu-50/50, and the molecular weight was computed to be 6284, while for OBB/PLu-80/20, the intrinsic viscosity was found to be 0.61 and M_w = 5620. The intrinsic viscosity for OBB/PLu-20/80 was calculated to be 0.42, and the molecular weight was found to be 3348. The oligomers were obtained by a free radical polymerization mechanism as per our previously reported works.[26,27] The monomers in the presence of ferric chloride undergo oxidation, which leads to the creation of a positive charge. The charged monomer then attacks either the same monomer or the co-monomer depending upon the reactivity ratios of the two monomers. The chemical polymerization of conducting polymers is usually carried out in an acidic medium to ensure doping of anions on the polymer chains. In our case, ferric chloride was used as an oxidant and is also reported to serve as a dopant in the presence of an acidic medium, and hence the chains obtained were those of Cl-doped oligomers as shown in Scheme 1.

Optimization of the Geometries of Oligomers via DFT for Determination of Vibrational and Electronic Spectra and Analysis of Mulliken Charge and HOMO−LUMO Energies. The geometrical structures of the oligomers were optimized by taking one monomeric unit of BB and two units of luminol for OBB/PLu-20/80, one monomeric unit each of BB and luminol for OBB/PLu-50/50, and two monomeric units of BB with one monomeric unit of luminol for OBB/PLu-80/20. For pristine luminol, a trimer unit was taken for the geometry optimization (figures provided in the Supporting Information as Figure S1a−h). The optimized geometry of PLu oligomer was noticed to be non-planar, and the charge distribution was around the ring containing oxygen as well as amide groups. The optimized geometry of OBB/PLu-20/80 was noticed to be planar, and the charge distribution was mainly around the amino groups at the terminal aromatic ring of BB as well as on the luminol units. The optimized geometry of OBB/PLu-50/50 appeared to be twisted around the luminol units of the oligomer, and the

https://doi.org/10.1021/acsomega.1c03459
ACS Omega 2021, 6, 27833−27841

charge was seen to be concentrated around the carbonyl and amide groups of luminol and also around the amino groups at the terminal aromatic ring of BB. Interestingly, the optimized geometry of OBB/PLu-80/20 was noticed to be highly planar among all oligomers and the charge was noticed to be highly dense at the amino linkages.

The highest occupied molecular orbitals of PLu (Figure 1a) were found to be evenly distributed over the backbone of the BB unit in the oligomer. The lowest unoccupied molecular orbitals appeared to be less symmetrical, which were also distributed along the BB unit. The HOMO−LUMO energy was computed to be 5.74 eV for PLu. In the oligomer OBB/PLu-20/80 (Figure 1b), the lowest unoccupied molecular orbitals were noticed to be distributed uniformly over the entire backbone of the oligomer, while the highest occupied molecular orbitals were noticed to be concentrated around the linkage of luminol and the BB unit. The HOMO−LUMO energy was calculated to be 1.65 eV in this case. However, in the case of OBB/PLu-50/50 (Figure 1c), the LUMO energy is found to be about 2 eV. The lowest unoccupied molecular orbitals appear to be symmetric over the most part of the backbone of the oligomer. OBB/PLu-80/20 in Figure 1d revealed a highly symmetric distribution of the lowest unoccupied molecular orbitals and the HOMO−LUMO energy was computed to be 1.29 eV.

Experimental and Theoretical IR Analysis. The IR spectrum of pristine PLu (Table 1 and Supporting Information, Figure S2a−d) revealed that the NH stretching vibration peak at 3355 cm^{-1} was due to the presence of a secondary amine, while the theoretical spectrum revealed the NH stretching vibration peak at 3350 cm^{-1}. The peaks associated with benzenoid and quinonoid rings appeared at 1587, 1492, and 1326 cm^{-1}, while the theoretical spectrum exhibited the same peaks at 1590, 1480, 1485, 1350, and 1320 cm^{-1}. The CN stretching vibration was observed at 1234 cm^{-1}. The C−H bending vibration peak was found at 1110 cm^{-1}, while the peaks at 995 and 793 cm^{-1} were correlated to the presence of a substituted benzene ring and fused aniline ring of luminol.[20−22] The peaks of PLu were similar to the values reported in our previous studies[20,22] and therefore confirmed the polymerization of luminol.

The oligomer OBB/PLu-20/80 also revealed an NH stretching vibration peak at 3310 cm^{-1}, and the theoretical spectrum revealed the same peak at 3300 cm^{-1}. The imine stretching peak was noticed at 1624 and 1628 cm^{-1} in the experimental and theoretical spectrum, respectively. The quinonoid and benzenoid ring stretching vibration peaks were noticed at 1587, 1492, and 1336 cm^{-1}. The theoretical spectrum revealed the same peaks at 1589, 1488, 1378¯, and 1330 cm^{-1}. The CN stretching vibration peak appeared at 1234 cm^{-1} in the experimental spectrum, and the same vibration was seen at 1230 cm^{-1} in the theoretical spectrum. The substituted and fused aniline ring peaks were found to be in close agreement in the theoretical and experimental spectra. The oligomer OBB/PLu-50/50 revealed a shift of 34 cm^{-1} in the experimental spectrum, while the imine stretching peak showed a minor shift of 6 cm^{-1}. The quinonoid and benzenoid peaks showed a shift of 10 cm^{-1}, while the CN peak revealed a small shift of 4 cm^{-1}. The aromatic peaks, however, were found to be in close agreement. Similarly, the experimental IR spectrum of OBB/PLu-80/20 revealed peaks that were found to be in good agreement with the theoretical spectrum. The presence of the above peaks established the structure of the oligomers as shown in Scheme 1. Significant changes were noticed in the NH region of the oligomers due to the synergistic interaction between the two moieties.

Table 1. IR Spectral Data of PLu and OBB/PLu Oligomers

samples	functional group	wavenumber (cm^{-1})	wavenumber (cm^{-1}) (theoretical)
PLu	N−H stretching	3355	3350
	imine stretching	1610	1620
	C=C stretching (quinonoid)	1587 and 1492	1590, 1580, and 1485
	C=C stretching (benzenoid)	1326	1350 and 1320
	C−N stretching	1234	1230
	C−H bending	1110	1120 and 1110
	substituted benzene ring	995	990 and 930
	fused aniline ring of luminol	793	795
OBB/PLu-20/80	N−H stretching	3310	3300
	imine stretching	1624	1628
	C=C stretching (quinonoid)	1587 and 1492	1589 and 1488
	C=C stretching (benzenoid)	1336	1378 and 1330
	C−N stretching	1234	1230
	C−H bending	1109	1090
	substituted benzene ring	887	992
	fused aniline ring of luminol	790	793
OBB/PLu-50/50	N−H stretching	3334 and 3197	3300 and 3093
	imine stretching	1624	1630
	C=C stretching (quinonoid)	1473	1486
	C=C stretching (benzenoid)	1371 and 1324	1369 and 1347
	C−N Stretching	1220	1224
	C−H bending	1120	1090
	substituted benzene ring	887	990
	fused aniline ring of luminol	790	790
OBB/PLu-80/20	N−H stretching	3130	3110
	imine stretching	1610	1639 and 1618
	C=C stretching (quinonoid)	1587 and 1490	1590 and 1486
	C=C stretching (benzenoid)	1332 and 1319	1347 and 1323
	C−N stretching	1224	1224
	C−H bending	1051	1043
	substituted benzene ring	925	920
	aniline ring of luminol	786	790

Fluorescence and Confocal Analysis. The emission spectra of PLu and its co-oligomers with OBB are shown in Figure 2. The emission spectrum of PLu upon excitation at 350 nm revealed a peak at 420 nm, which has been reported in our previous studies and was correlated to the S_1−So transition.[20−22] However, upon loading of OBB (up to 20%), the emission spectrum revealed a redshift of 80 nm and was noticed at 500 nm. Similarly, the emission spectra of OBB/PLu-50/50 and OBB/PLu-80/20 revealed an intense but broad peak at 500 nm. The intensity of the peak was noticed

https://doi.org/10.1021/acsomega.1c03459
ACS Omega 2021, 6, 27833−27841

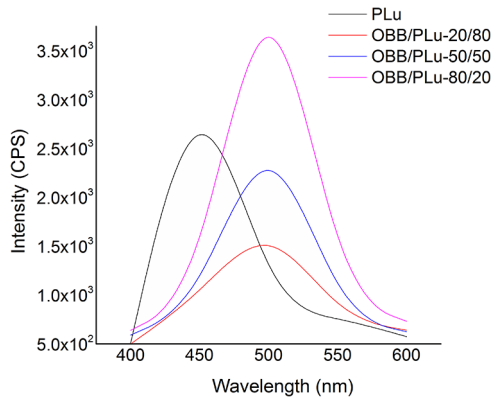

Figure 2. Fluorescence spectra of PLu and OBB/PLu oligomers.

to increase with the increase in the loading of OBB and was therefore associated with the emission peak of OBB. Quantum yield (φ) was calculated, taking rhodamine B (RhB) as a reference material.[20−22] The calculated φ values were obtained as 0.0010, 0.039, 0.048, and 0.081, revealing that the quantum yield increased with the increase in the OBB content in the oligomer (Table 2). These results displayed that the emission in the UV/visible range could be obtained by choosing the appropriate composition of the monomers in the oligomer.

Table 2. Quantum Yield of PLu and Its Oligomers with BB Dye

sample	λ_{max} (nm)	integrated area	quantum yield (φ)
PLu	400	1.20×10^3	0.0010
OBB/PLu-20/80	500	2.15×10^3	0.039
OBB/PLu-50/50	500	2.86×10^4	0.048
OBB/PLu-80/20	500	3.22×10^4	0.081

The confocal image of PLu in Figure 3a exhibited blue emission, which has been previously observed for PLu and its co-polymers.[20−22] The confocal image of OBB/PLu-20/80 and OBB/PLu-50/50 in Figure 3b,c showed scattered particles exhibiting red emission, while in the case of OBB/PLu-80/20 in Figure 3d, the intensity as well as the brightness of the red emission was noticed to be higher, thereby corroborating the results of the fluorescence studies that the increase in the emission intensity was attributed to the increase in the loading of OBB in the oligomer. The studies therefore confirmed that the fluorescence emission could be tuned to show red emission by controlling the OBB dye content in the oligomer.

Experimental and Theoretical UV−visible Studies. The UV−visible spectrum of PLu in Figure 4a revealed peaks at 290 and 420 nm. The 290 nm peak was associated with the $\pi-\pi^*$ transition, while the 420 nm peak was correlated to the $n-\pi^*$ transition as reported in our previous studies.[22−25] The same peaks appeared at 300 and 405 nm, respectively, in the theoretically computed spectrum. The experimental UV−visible spectrum of OBB/PLu-20/80 (Figure 4b) revealed peaks at 350 and 430 nm, whereas the theoretical spectrum revealed peaks at 350 and 450 nm. The peak around 430 nm in the experimental spectrum and 450 nm in the theoretical spectrum was attributed to the presence of OBB dye. The experimental UV spectrum of OBB/PLu-50/50 and OBB/PLu-80/20 (Figure 4c,d) also showed peaks at 350 and 450 nm, and the intensity of the peaks in the theoretical spectrum were noticed to be higher. Interestingly, the peak intensities corresponding to the 450 nm peak were noticed to increase with the increase in the content of OBB in the oligomer. The experimental oscillator strength values were calculated to be 0.17, 1.1, 0.9, and 1.6 for PLu, OBB/PLu-20/80, OBB/PLu-50/50, and OBB/PLu-80/20, respectively, which were in close agreement with the theoretical values in Table 3.

Morphological Studies. The SEM micrograph of PLu in Figure 5a showed a granular morphology forming agglomerates of various sizes. The SEM micrograph of OBB/PLu-20/80 in Figure 5b also revealed a granular structure predominantly resembling pristine PLu, while the SEM micrograph of OBB/PLu-50/50 in Figure 5c exhibited a layered morphology, revealing bright agglomerates. The morphology of OBB/PLu-80/20 in Figure 5d showed formation of an intense granular structure with tiny grains stacked together. The morphology was noticed to undergo a major transformation upon increasing the loading of OBB in PLu. The results revealed that the content of PLu/OBB had a significant impact on the morphological features as well besides the electronic properties, and the loading of the either moieties could be easily identified via the drastic change from dense bright cluster formation to dark granular agglomerate formation.

Sensing Studies of Li^+ Ions. Recently, in the field of metal sensing, polymers have become more and more important owing to some advantages like easy fabrication and signal amplification compared to a simple organic compound. We have carried out spectrophotometric determination of Li^+ ions using LiCl salt and a Li_2CO_3 drug, which is highly used in psychiatric treatment. Dilute solutions of oligomers OBB/PLu-20/80 and OBB/PLu-80/20 (5.0×10^{-6} M) were taken, and LiCl/Li_2CO_3 drug solution (2.5×10^{-3} M) was added to the polymer solution to record the change in the peak intensities of the oligomers. Upon progressive addition of Li^+ ion solution to the oligomers, the absorption intensities were noticed to decrease with the increase in the concentration of the Li^+ ions (figures provided in the Supporting Information as Figure S3a−f). The absorbance change $(A_o - A_{420})/A_o$ at 420 nm showed a gradual decrease with the increase in the Li^+ ion concentration. The fitting curve showed an excellent change in absorbance with concentration, thereby depicting linear detection with an R^2 value of 0.9978 (figures provided in the Supporting Information as Figure S4a−c). The detection limit (LOD) of OBB and its oligomers with PLu was calculated and is shown in Figure 6. The LOD values were computed to be 5.1×10^{-6} M, 5.6×10^{-6} M, and 7×10^{-6} M for OBB, OBB/PLu-20/80, and OBB/PLu-80/20, respectively. The values were found to be acceptable for designing these oligomers as probes in the detection of Li.

CONCLUSIONS

Oligomers of PLu were synthesized using different loadings of the dye and luminol with a view to design conjugated oligomers for their application in sensing devices. The loading of BB dye as well as luminol was established via experimental and theoretical IR as well as UV studies. The surface morphology of oligomers was found to be dependent on the loading of luminol as well as BB. The quantum yield (φ) values were found to increase with the increase in the loading of the BB dye. The HOMO−LUMO energy was found to decrease with the increase in the loading of dye.

https://doi.org/10.1021/acsomega.1c03459
ACS Omega 2021, 6, 27833−27841

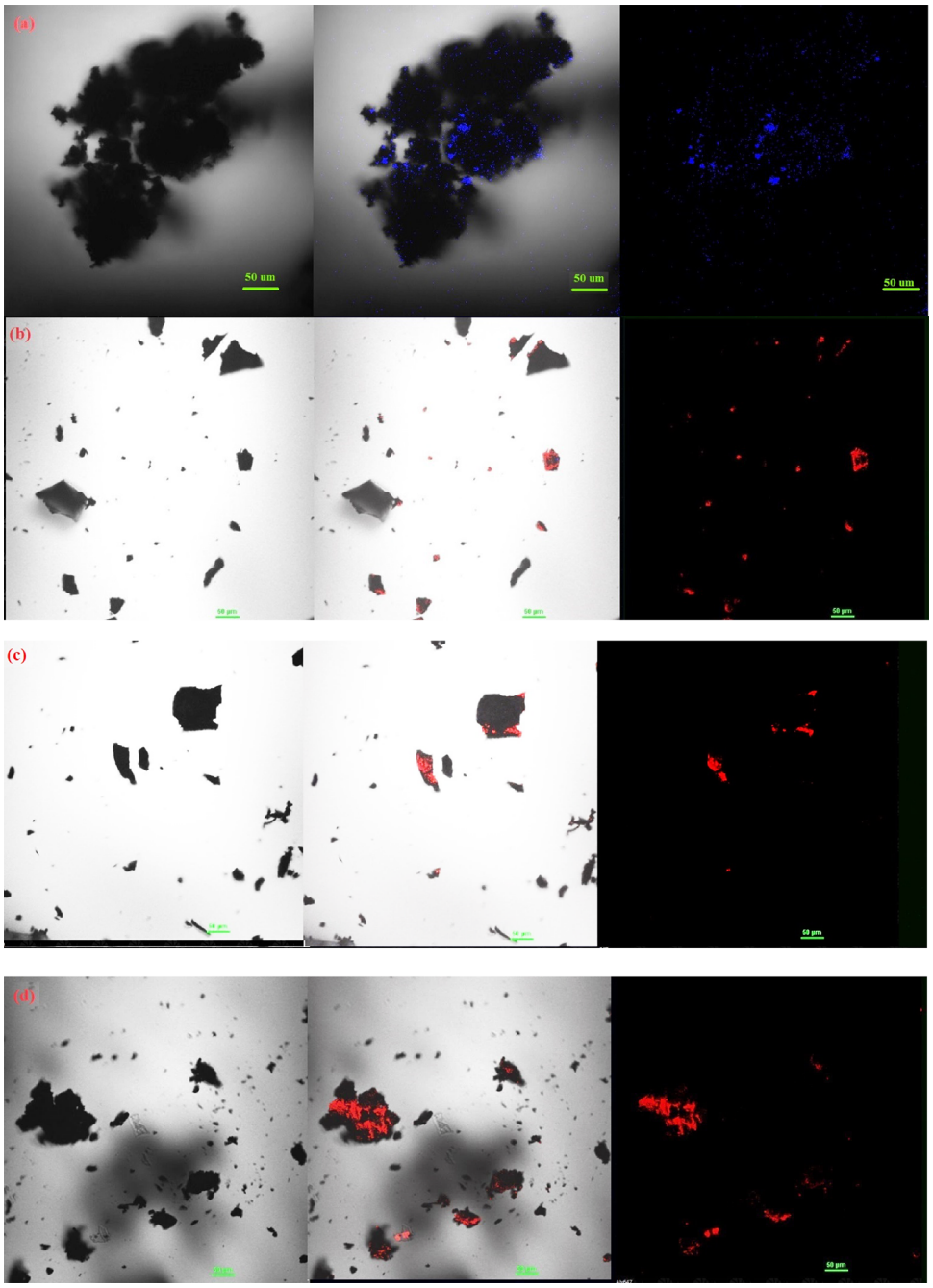

Figure 3. Confocal images of (a) PLu, (b) OBB/PLu-20/80, (c) OBB/PLu-50/50, and (d) OBB/PLu-80/20.

Spectrophotometric determination of a Li_2CO_3 drug confirmed the lowest limit of detection to be 5.1×10^{-6} M, which was good enough to design sensing probes for Li^+ ion detection in real samples. Studies on the detection of lithium in blood samples are underway and shall be published soon.

EXPERIMENTAL SECTION

Bismarck Brown dye (SD Fine Chem Ltd., India), luminol (Sigma Aldrich, USA), ferric chloride (Merck, India), hydrochloric acid (Merck, India), *N*-*N*-dimethyl pyrrolidone (NMP) (Merck, India), dimethyl formamide (DMF), and distilled water were used without further purification.

Polymerization of Luminol with Bismarck Brown Dye. Bismarck Brown dye (BB) (1 g, 2.3×10^{-3} mol) was dissolved in an aqueous solution of 2 M HCl (25 mL), and luminol (Lu) (1 g, 5.6×10^{-3} mol) dissolved in DMF (5 mL) was added to a 250 mL Erlenmeyer flask. The solution was stirred at 25 °C for 20 min. Ferric chloride (1 g, 6.0×10^{-3} mol) dissolved in distilled water (25 mL) was added to the reaction mixture and further stirred on a magnetic stirrer for 2 h at −5 °C. The obtained product was kept in a deep freezer for 24 h. The removal of unreacted ferric chloride was ensured by washing several times with distilled water and testing the filtrate for the presence of Fe ions using potassium ferrocyanide as per the reported method.[27] The obtained product was isolated via Soxhlet extraction and then dried in a vacuum oven for 72 h at 70 °C to ensure complete removal of water and impurities. The obtained oligomer was designated as OBB/PLu-20/80 based on the molar ratio taken for synthesis. A similar procedure was adopted for the

https://doi.org/10.1021/acsomega.1c03459
ACS Omega 2021, 6, 27833−27841

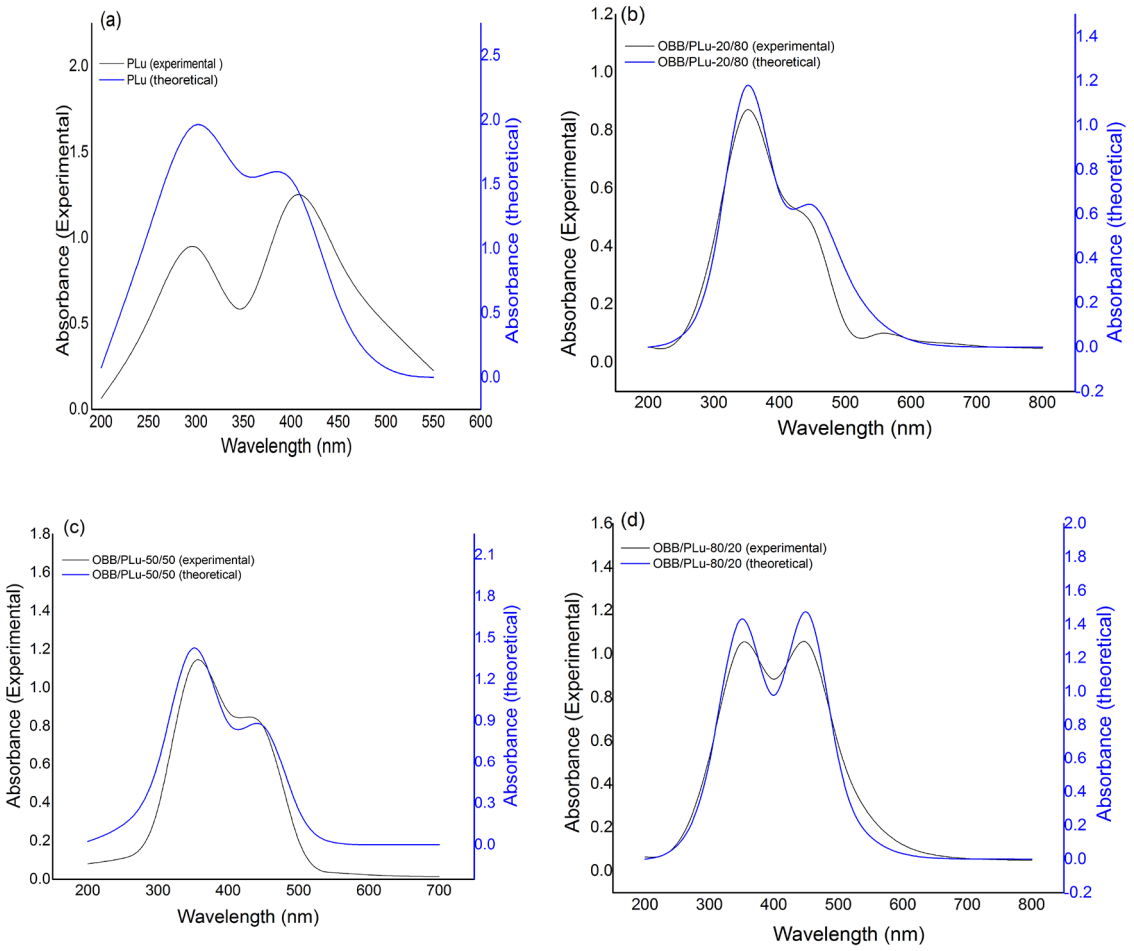

Figure 4. UV−visible spectra of (a) PLu, (b) OBB/PLu-20/80, (c) OBB/PLu-50/50, and (d) OBB/PLu-80/20.

Table 3. Oscillator Strength of PLu and OBB/PLu Oligomers

polymer/co-polymer	λ_{max}, experimental (theoretical)	oscillator strength, experimental (theoretical)
PLu	420 (405)	0.17 (0.18)
OBB/PLu-20/80	430 (450)	1.1 (1.2)
OBB/PLu-50/50	450 (450)	0.9 (1.1)
PBB/PLu-80/20	450 (450)	1.6 (1.8)

oligomerization of OBB/PLu-80/20, OBB/PLu-50/50, and pure luminol, which was designated as PLu.

CHARACTERIZATION

Spectral Studies. IR measurements were carried out on a Fourier transform infrared (FTIR) spectrophotometer model Shimadzu IRA Affinity−1 in the form of KBr pellets. UV−visible spectra were taken on a Perkin-Elmer-Lamda-Ez-25 by dissolving the oligomers in NMP. Fluorescence spectra of the sample were taken in solution form (NMP solvent) and recorded on a fluorescence spectrophotometer model Horiba Fluorolog @ 3-11.

Morphological Studies. SEM images were taken on a field emission-scanning electron microscope (FE-SEM, Leo Supra 50VP, Carl Zeiss, Germany) equipped with an energy-dispersive X-ray system. Fluorescence images were obtained using a laser confocal microscope with a fluorescence correlation spectroscope (Olympus FluoView FV1000) equipped with a He−Ne laser and oil immersion objective.

Theoretical Studies. DFT and TD-DFT calculations were performed using GAUSSIAN 09 software, and the optimized geometries were obtained using the DFT/B3LYP method with the 6-311G(d) basis set.[21,25] The oscillator strength, HOMO−LUMO energies, and band gap were determined using the optimized geometries with the same basis set. The same optimized structures were used in the vibrational frequency calculations. The UV−vis spectra of geometry-optimized structures were simulated at TD-DFT/B3LYP using the 6-311G(d) basis set.

Sensing Studies of Li^+ Ions in Solution. We employed DMF solutions to perform UV titration experiments. The stock solutions (100 μL) comprised deionized water containing LiCl and a Li_2CO_3 drug. The oligomer solution (5×10^{-6} M) was prepared in DMF. The LiCl and Li_2CO_3 stock solutions (2.5×10^{-5} M) were prepared by dissolving an appropriate amount of salt in DMF (0.00035 g, 5×10^{-6} M). The salt solution was then added to the oligomer solutions (200 μL) in various concentrations ranging from 10 to 100 μL, and the UV−visible spectra were recorded in a wavelength range of 300−800 nm.

The detection limit for Li^+ ions by the oligomer was calculated based on IUPAC 3σ criteria using a UV/vis spectrophotometer with a 1 cm path-length cuvette. A blank solution of oligomer (5×10^{-6} M) in DMF was scanned at least five times to determine the standard deviation of the

https://doi.org/10.1021/acsomega.1c03459
ACS Omega 2021, 6, 27833−27841

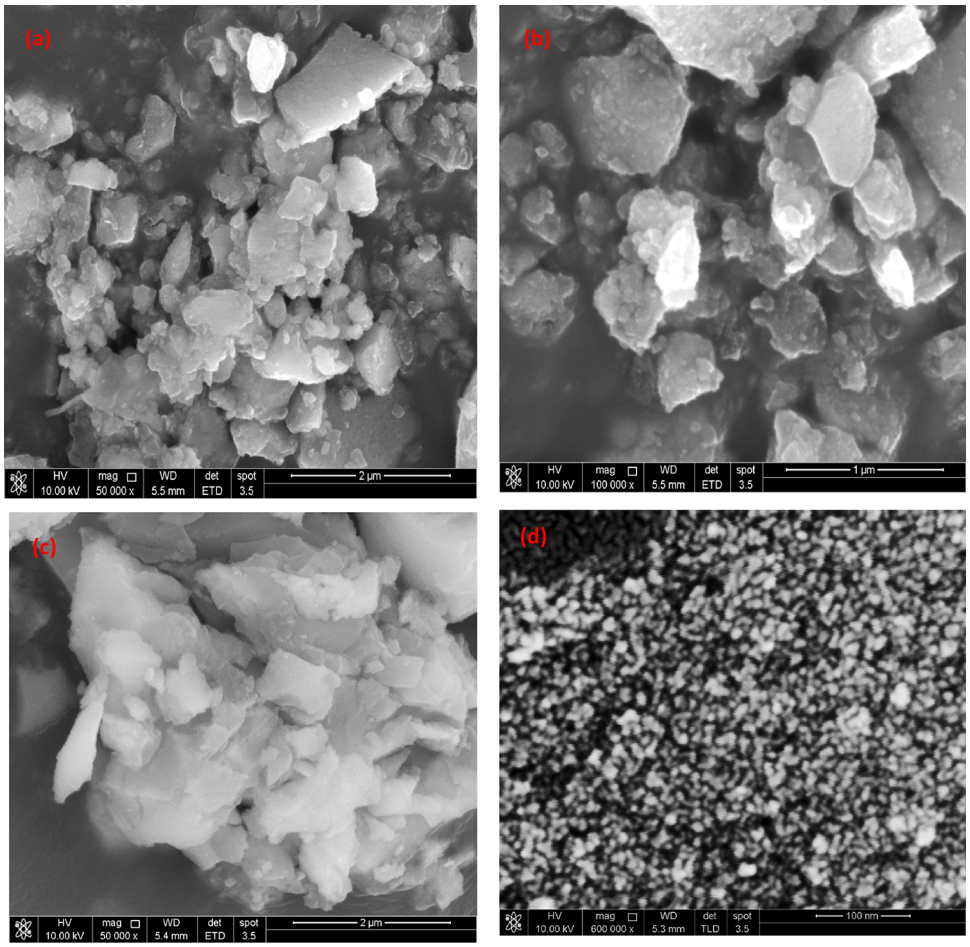

Figure 5. SEM micrographs of (a) PLu (mag: 50,000×), (b) OBB/PLu-20/80 (mag: 100,000×), (c) OBB/PLu-50/50 (mag: 50,000×), and (d) OBB/PLu-80/20 (mag: 50,000×).

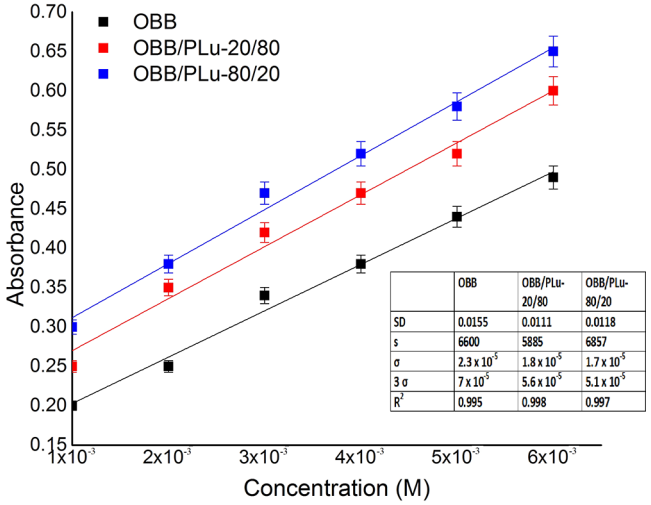

	OBB	OBB/PLu-20/80	OBB/PLu-80/20
SD	0.0155	0.0111	0.0118
s	6600	5885	6857
σ	2.3×10^{-5}	1.8×10^{-5}	1.7×10^{-5}
3 σ	7×10^{-5}	5.6×10^{-5}	5.1×10^{-5}
R^2	0.995	0.998	0.997

Figure 6. LOD values of OBB and its oligomers.

blank. The same solution was then titrated with Li^+ ions (2.5×10^{-3} M). After each addition, the solution was shaken and then incubated for 3 min before scanning at room temperature. A linear calibration curve was established by plotting the absorbance against the concentration of Li^+ ions. The LOD was calculated using the equations LOD = 3σ and σ = SD/s, where SD is the standard deviation of the blank oligomer solution and s is the slope of the calibration curve.

■ ASSOCIATED CONTENT

Supporting Information

The Supporting Information is available free of charge at https://pubs.acs.org/doi/10.1021/acsomega.1c03459.

(Table S1) Solubility test of polymers and co-polymers; (Figure S1) optimized geometry of PLu, Mulliken charge distribution in PLu, optimized geometry of OBB/PLu-20/80, Mulliken charge distribution in OBB/PLu-20/80, optimized geometry of OBB/PLu-50/50, Mulliken charge distribution in OBB/PLu-50/50, optimized geometry of OBB/PLu-80/20, and Mulliken charge distribution in OBB/PLu-80/20; (Figure S2) FTIR spectra of PLu, OBB/PLU-20/80, OBB/PLu-50/50, and OBB/PLU-60/20; (Figure S3) UV spectra depicting change in absorbance of OBB and its oligomers with PLu upon addition of lithium chloride and lithium carbonate; (Figure S4) relationship between absorbance change and concentrations of Li^+ ions in lithium chloride and lithium carbonate using OBB, OBB/PLu-20/80, and OBB/PLu-80/20 (PDF)

https://doi.org/10.1021/acsomega.1c03459
ACS Omega 2021, 6, 27833−27841

AUTHOR INFORMATION

Corresponding Author

Ufana Riaz − *Materials Research Laboratory, Department of Chemistry, Jamia Millia Islamia, New Delhi 110025, India;* orcid.org/0000-0001-7485-4103; Email: ufana2002@yahoo.co.in

Authors

Neetika Singh − *Materials Research Laboratory, Department of Chemistry, Jamia Millia Islamia, New Delhi 110025, India;* orcid.org/0000-0002-4553-5194

Elham S. Aazam − *Chemistry Department, Faculty of Science, King Abdul Aziz University, Jeddah 23622, Saudia Arabia*

Complete contact information is available at: https://pubs.acs.org/10.1021/acsomega.1c03459

Author Contributions

The manuscript was written through contributions of all authors. All authors have given approval to the final version of the manuscript. U.R. conceptualized the work and analyzed the results while N.S. carried out the experimental studies, and E.S.A. contributed in analyzing and interpreting morphological studies.

Notes

The authors declare no competing financial interest.

ACKNOWLEDGMENTS

The authors wish to acknowledge the DST-PURSE, Jamia Millia Islamia (JMI), New Delhi-110025, India, for providing the instrumentation facility. N.S. wishes to acknowledge the RGNF-SRF, UGC, India, for providing funding support to conduct this research work.

REFERENCES

(1) Dey, A.; Singh, A.; Das, D.; Iyer, P.K.Organic Semiconductors: A New Future of Nanodevices and Applications. In *Thin Film Structures in Energy Applications*; Springer International Publishing: Cham, 2015, 97−128.

(2) Costa, C.; Farinhas, J.; Avó, J.; Morgado, J.; Galvão, A. M.; Charas, A. Structural Dependence of the Optical Properties of Narrow Band Gap Thiophene−Thiadiazoloquinoxaline Derivatives and Their Application in Organic Photovoltaic Cells. *New J. Chem.* **2019**, *43*, 5202−5213.

(3) Lee, J.; Kalin, A. J.; Yuan, T.; Al-Hashimi, M.; Fang, L. Fully Conjugated Ladder Polymers. *Chem. Sci.* **2017**, *8*, 2503−2521.

(4) Porcarelli, L.; Shaplov, A. S.; Bella, F.; Nair, J. R.; Mecerreyes, D.; Gerbaldi, C. Single-Ion Conducting Polymer Electrolytes for Lithium Metal Polymer Batteries that Operate at Ambient Temperature. *ACS Energy Lett.* **2016**, *1*, 678−682.

(5) Ramya, R.; Sivasubramanian, R.; Sangaranarayanan, M. V. Conducting polymers-based electrochemical supercapacitors—Progress and prospects. *Electrochim. Acta* **2013**, *101*, 109−129.

(6) Kausar, A. High-performance competence of polyaniline-based nanomaterials. *Mater. Res. Innovations* **2020**, *24*, 113−122.

(7) Dakshayini, B. S.; Reddy, K. R.; Mishra, A.; Shetti, N. P.; Malode, S. J.; Basu, S.; Naveen, S.; Raghu, A. V. Role of conducting polymer and metal oxide-based hybrids for applications in ampereometric sensors and biosensors. *Microchem. J.* **2019**, *147*, 7−24.

(8) Guo, Y.; Zhou, X.; Zhao, F.; Bae, J.; Rosenberger, B.; Yu, G. Synergistic Energy Nanoconfinement and Water Activation in Hydrogels for Efficient Solar Water Desalination. *ACS Nano* **2019**, *13*, 7913−7919.

(9) Riaz, U.; Singh, N.; Verma, A.; Aazam, E. S. Studies on conducting polymer intercalated layered double hydroxide nanocomposites: Anti-tuberculosis drug delivery agents. *Polym. Eng. Sci.* **2020**, *60*, 2628−2639.

(10) Wanga, D.; Lu, C.; Zhao, J.; Han, S.; Wua, M.; Chen, W. High energy conversion efficiency conducting polymer actuators based on PEDOT:PSS/MWCNTs composite electrode. *RSC Adv.* **2017**, *7*, 31264−31271.

(11) Naveen, M. H.; Gurudatt, N. G.; Shim, Y.-B. Applications of conducting polymer composites to electrochemical sensors: A review. *Appl. Mater. Today* **2017**, *9*, 419−433.

(12) Li, X.; Zheng, Y.; Li, C. Multicolored Polyanilines Doped by Different Acid Dyes and Their Electrochromic Property. *MATEC Web Conf.* **2016**, *67*, No. 06025.

(13) Riaz, U.; Singh, N. Facile Synthesis of Malachite Green Incorporated Conducting Polymers: A Comparison of Theoretical and Experimental Studies. *Synth. Met.* **2019**, *257*, 116184.

(14) Qiu, F.; Cao, Y.; Xu, H.; Jiang, Y.; Zhou, Y.; Liu, J. Synthesis and Properties of Polymer Containing Azo-Dye Chromophores for Nonlinear Optical Applications. *Dyes Pigm.* **2007**, *75*, 454−459.

(15) Valtera, S.; Prokeš, J.; Kopecká, J.; Vrňata, M.; Trchová, M.; Varga, M.; Stejskal, J.; Kopecký, D. Dye-Stimulated Control of Conducting Polypyrrole Morphology. *RSC Adv.* **2017**, *7*, 51495−51505.

(16) Lei, T.; Wang, J.-Y.; Pei, J. Design, Synthesis, and Structure−Property Relationships of Isoindigo-Based Conjugated Polymers. *Acc. Chem. Res.* **2014**, *47*, 1117−1126.

(17) Kaur, A.; Cazeca, M. J.; Chittibabu, K. G.; Kumar, J.; Tripathy, S. K. Mechanism of Electroluminescence in Dye Doped Thiophene Based Conjugated Polymer. *J. Appl. Phys.* **2001**, *89*, 3250−3255.

(18) Hsu, S. L.; Chen, C. M.; Wei, K. H. Carbazole-Based Conjugated Polymers Incorporating Push/Pull Organic Dyes: Synthesis, Characterization, and Photovoltaic Applications. *J. Polym. Sci., Part A: Polym. Chem.* **2010**, *48*, 5126−5134.

(19) Jung, E. H.; Ahn, H.; Jo, W. H.; Jo, J. W.; Jung, J. W. Isoindigo-Based Conjugated Polymer for High-Performance Organic Solar Cell with a High VOC of 1.06 V as Processed from Non-Halogenated Solvent. *Dyes Pigm.* **2019**, *161*, 113−118.

(20) Riaz, U.; Jadoun, S.; Kumar, P.; Kumar, R.; Yadav, N. Microwave-Assisted Facile Synthesis of Poly(Luminol-*Co*-Phenylenediamine) Copolymers and Their Potential Application in Biomedical Imaging. *RSC Adv.* **2018**, *8*, 37165−37175.

(21) Jadoun, S.; Verma, A.; Riaz, U. Luminol modified polycarbazole and poly(*o*-anisidine): Theoretical insights compared with experimental data. *Spectrochim. Acta, Part A* **2018**, *204*, 64−72.

(22) Jadoun, S.; Sharma, V.; Ashraf, S. M.; Riaz, U. Sonolytic Doping of Poly(1-Naphthylamine) with Luminol: Influence on Spectral, Morphological and Fluorescent Characteristics. *Colloid Polym. Sci.* **2017**, *295*, 715−724.

(23) Singh, N.; Kumar, P.; Kumar, R.; Aazam, E. S.; Riaz, U. Development of a near Infrared Novel Bioimaging Agent *via* Co-Oligomerization of Congo Red with Aniline and *o*-Phenylenediamine: Experimental and Theoretical Studies. *RSC Adv.* **2019**, *9*, 36479−36491.

(24) Qassem, M.; Triantis, I.; Hickey, M.; Palazidou, E.; Kyriacou, P. Methodology for rapid assessment of blood lithium levels in ultramicro volumes of blood plasma for applications in personal monitoring of patients with bipolar mood disorder. *J. Biomed. Opt.* **2018**, *23*, 1−6.

(25) Singh, N.; Arish, M.; Kumar, P.; Rub, A.; Riaz, U. Experimental and Theoretical Studies of Novel Azo Benzene Functionalized Conjugated Polymers: *In-vitro* Antileishmanial Activity and Bioimaging. *Sci. Rep.* **2020**, *10*, 57−67.

(26) Riaz, U.; Ashraf, S. M.; Aleem, S.; Budhiraja, V.; Jadoun, S. Microwave-Assisted Green Synthesis of Some Nanoconjugated Copolymers: Characterisation and Fluorescence Quenching Studies with Bovine Serum Albumin. *New J. Chem.* **2016**, *40*, 4643−4653.

(27) Jadoun, S.; Ashraf, S. M.; Riaz, U. Tuning the spectral, thermal and fluorescent properties of conjugated polymers via random copolymerization of hole transporting monomers. *RSC Adv.* **2017**, *7*, 32757−32768.